

The mechanical properties of rock salt under cyclic loading-unloading experiments

Jie Chen ^{*1}, Chao Du ², Deyi Jiang ¹, Jinyang Fan ¹ and Yi He ¹

¹ State Key Laboratory of Coal Mine Disaster Dynamics and Controls,
Chongqing University, Chongqing 400030, China

² China Southwest Geotechnical Investigation & Design Institute CO., LTD., 610052 Chengdu, China

(Received April 23, 2015, Revised December 25, 2015, Accepted December 29, 2015)

Abstract. Rock salt is a near-perfect material for gas storage repositories due to its excellent ductility and low permeability. Gas storage in rock salt layers during gas injection and gas production causes the stress redistribution surrounding the cavity. The triaxial cyclic loading and unloading tests for rock salt were performed in this paper. The elastic-plastic deformation behaviour of rock salt under cyclic loading was observed. Rock salt experienced strain hardening during the initial loading, and the irreversible deformation was large under low stress station, meanwhile the residual stress became larger along with the increase of deviatoric stress. Confining pressure had a significant effect on the unloading modulus for the variation of mechanical parameters. Based on the theory of elastic-plastic damage mechanics, the evolution of damage during cyclic loading and unloading under various confining pressure was described.

Keywords: rock salt; triaxial; cyclic loading-unloading; deformation; damage

1. Introduction

During gas injection and production in salt cavern, the gas pressure changing makes the stress redistribution surrounding rock, just like the rock salt experiences cyclic loading. Under the effects of cyclic loading and unloading, a variable stress state will develop around the cavity and cause shear dilatation. Micro-cracks inside the rock form and expand constantly, causing continual damage, and an excavation damage zone will form around the cavity (Kwon *et al.* 2009, Alkan 2009). In the excavation damage zone, the hydraulic properties of the rock salt will change greatly and the permeability will increase by several time orders (Wang and Zhang 2014a); this may pose a serious threat to the functionality and effectiveness of geological gas storage in rock salt.

At present, many reports on the mechanical characteristics of rock under uniaxial cyclic loading have appeared, such as the deformations and strength of rocks (Li *et al.* 2014, Závada *et al.* 2015), the acoustic emission phenomenon of rocks (Chen *et al.* 2015), and other parameters that reflect the mechanical properties of rocks under stress. The effects of damage in rocks on mechanical properties are quantified by the strain and the elastic modulus, the Felicity ratio and the load-unload response ratio, which are determined from methods including uniaxial compression and

*Corresponding author, Ph.D., E-mail: chenjie_cqu@163.com

different frequencies of uniaxial cyclic loading and unloading (Zhang *et al.* 2012, Wang *et al.* 2014c, Wang *et al.* 2014a, b, Wisetsaen *et al.* 2015).

Studies regarding the mechanical characteristics of rock under triaxial cyclic unloading-loading have also been published. In particular, researchers have investigated the residual strength of rock samples under different confining pressures and cyclic loading and unloading conditions (Ma *et al.* 2013). Ezersky and Goretsky (2014) measured velocity–resistivity versus porosity–permeability inter-relations in Dead Sea salt samples.

Compared to other rocks, the mechanical characteristics of rock salt are mainly manifested in plastic deformation features, expansion deformation, strain hardening characteristics and fatigue properties (Ren *et al.* 2013, Guo *et al.* 2012). Alkan *et al.* (2007) combined acoustic emission and triaxial compression tests and described how the dilatant stress domain gives rise to the generation and propagation of cracks and to the increase of damage with strain. Based on the damage of rock salt, Zhou *et al.* (2013) concluded that low frequency cyclical loading and unloading methods have time dependent effects and can accurately reproduce the observed damage characteristics. Fuenkajornet and Phueakphum (2010) studied the effects of cyclic loading on compressive strength, elasticity and time-dependent deformation.

The existing studies on cyclic loading and unloading of rock salt mostly focus on uniaxial compression tests, while experimental studies with triaxial compression cyclic loading and unloading are relatively neglected in the literature. This paper investigates the damage mechanic of rock salt under cyclic loading and unloading. Uniaxial compression and triaxial compression tests under constant confining pressure were performed on Jintan rock salt. The results were used to analyse the changes in deformation, Young's modulus, and the evolution of the damage process during loading and unloading.

2. Test procedure

The rock cores used in the experiments were taken from the Jintan Salt Mine, Jiangsu province, China (Liu *et al.* 2015). These cores are 100~103 mm in diameter and were drilled from a buried depth of 800~1200 m. Samples were prepared by dry machining with a machine tool, and cores were cut for buffering using a machine tool and a hacksaw. Then a machine tool was used for superfine machining at the end of the specimen and at the surface of the sample after cutting. The samples were 50 mm × 100 mm cylinders. The samples were wrapped with cling film after preparation and placed in a storage room until use. The samples after processing are shown in Fig. 1.

Uniaxial and triaxial cyclic loading and unloading tests were performed using the RMT-150C Rock Mechanics Testing System developed by the Rock and Soil Mechanics Division of the Chinese Academy of Sciences. The RMT-150C Rock Mechanics Testing System is a digitally controlled electro-hydraulic servo testing machine primarily used for the determination of the mechanical properties of rock and concrete materials. It can be used for uniaxial compression, uniaxial indirect tensile, triaxial compression and shear and other tests. The loading and control system of the testing machine is shown in Fig. 2.

Based on the dilatancy and hydraulic fracturing criteria of the stability evaluation, for German gas storage, the maximum internal pressure gradient is 0.015-0.02 MPa/m and the maximum and minimum pressure ratio is 2:1 and 6:1, determined empirically. Considering economics and safety, the Jintan gas storage system was built in the salt layers at approximately 1000 meters depth; the



50 mm × 100 mm cylinders

Fig. 1 Rock salt samples



Fig. 2 Rock Mechanical Test System (RMT)

internal pressure of the gas storage during operation was proposed to be between 6 MPa and 17 MPa. Gas injection and pumping causes stress redistribution surrounding the gas storage. To simulate the operation process, particularly considering six kinds of pressure conditions that the gas storage experiences during operation gas pressure from the maximum pressure drop to minimum pressure in a short time. Test were performed under 0, 5, 7, 10, 15 and 20 MPa confining pressure for both loading and unloading tests. The confining pressure adding rate is 0.1 MPa/s until to the set value. Using force control, apply axial compression at a rate of approximately 0.2 kN/s. The deviatoric stress was 5 MPa between loading and unloading.

3. The test results and analysis

The results of the executed tests for rock salt under six confining pressure loading and unloading conditions are shown as the stress-strain curve in Fig. 3. The detailed deformation characteristics of rock salt in the loading and unloading tests are shown in Table 1.

Figs. 4 and 5 show the loading and unloading stress-strain curves for rock salt under uniaxial and 5 MPa confining pressure conditions, respectively. Cyclic loading and unloading of rock samples gives an outer envelope curve that inosculates with the monotonic complete loading stress-strain curve. Although the maximum compressive strength of rock salt is 21.3 MPa, irreversible deformation accounts for 72.33% of the total deformation under 5 MPa unloading conditions. As shown in Table 1, with the growth of the displacement, plastic deformation of rock salt becomes more pronounced, and the proportion of irreversible deformation increases. For the unloading of 5, 10, 15 and 20 MPa conditions, the irreversible deformation accounted for 72%,

Table 1 Detailed deformation characteristics of rock salt under axial loading/unloading ($\sigma_3 = 5$ MPa)

Cycle order deformation/%	First	Second	Third	Fourth
The irreversible deformation ε'	0.077	0.167	0.401	0.873
The total deformation ε	0.106	0.221	0.477	0.990
ε'/ε 100	72	75	84	88

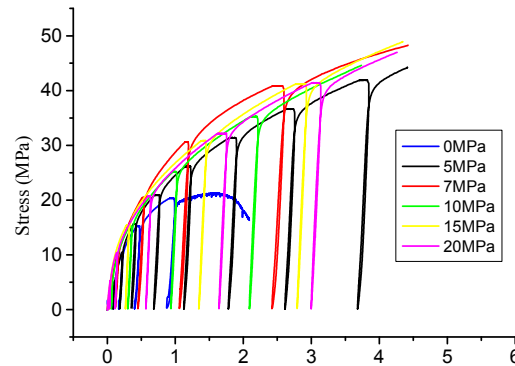


Fig. 3 The loading/unloading stress-strain curves of rock salt under different confining pressures

75%, 84% and 88% of the total deformation, respectively. The proportion of elastic strain: total strain (inelastic strain : total strain) are different during different deformation stages. The initial nonlinear strain from the beginning of loading, which may be due to generates micro-cracks or the original structure during core drilling and sample machining. Therefore, during the test, preloading of the rock samples with hydrostatic pressure was conducted to close these micro-cracks in the samples.

The slope of the initial loading curve is much smaller than that at the end of loading. Residual deformation after initial unloading is more than the residual deformation at the end of loading, which is associated with micro-crack closure and slip. In drilling and processing, the micro-cracks are developed. The structure of the sample before test is different from the rock salt 1000 m underground. The compaction stage at the initial loading procedure is usually short due to the micro-crack sliding and inelastic deformation. The inelastic strain is concentrated on grain boundaries in high stress concentration zones and crack tips. Rock salt experienced strain hardening during the initial loading. Therefore, the influence of subsequent loading on the inelastic deformation decreased significantly.

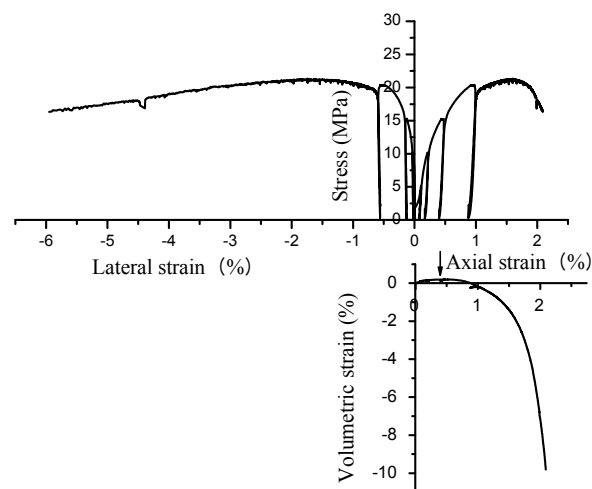


Fig. 4 The loading/unloading stress-strain curves of rock salt under axial compression

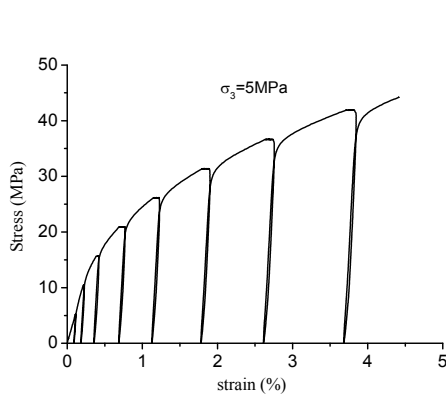


Fig. 5 Stress-strain curve of rock salt under the confining pressure 5 MPa

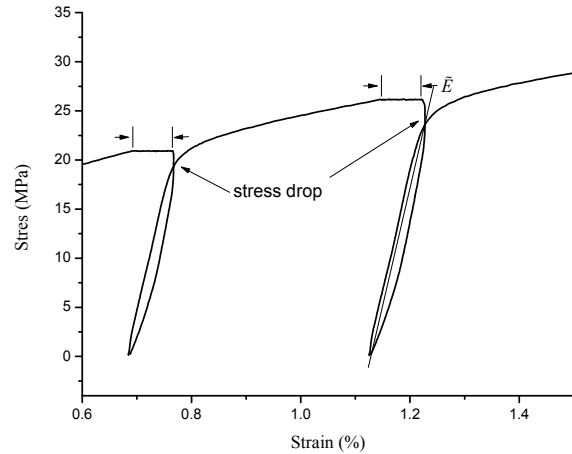


Fig. 6 Partial enlargement of a stress-strain curve of rock salt under 5 MPa confining pressure

In Fig. 6, the rock salt stress-strain curve in the loading and unloading cycle is shaped like an enclosed loop. Before each unloading event, the curve has a short horizontal line. This is because during manual operation, time elapses between the cessation of loading and preparation for unloading, so the axial load remains constant, resulting in rheological strain. The unloading process is typically nonlinear, while the reloading process is typically linear. Rock sample loading and unloading paths cannot be completely duplicated. The loading and unloading stress-strain curve always has a hysteresis loop. In purely elastic material, the paths between loading and unloading completely overlap, but the path between loading and unloading of viscoelastic materials is different. Rock salt stress-strain curves exhibit hysteresis loops under low stress, which reflects the strong viscous properties of rock salt.

When unloading, the friction between cracks will restrain the spring back of material and maintain residual stress. Therefore, at the beginning of each unloading event, a small amount of

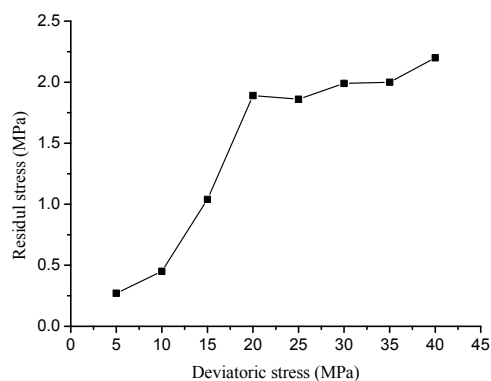


Fig. 7 Residual stress evolution of loaded/unloaded rock salt under 5 MPa confining pressure

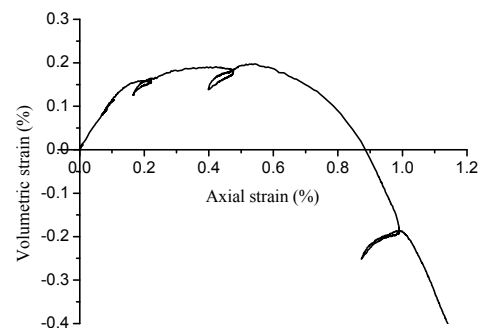


Fig. 8 The volumetric strain-axial strain curve of rock salt

strain remains unchanged, while the stress decreases linearly, the stress relaxation happened (the circle part in Fig. 6). The stress drop of the stress relaxation stage can be used as a measurement of the residual stress. As shown in Fig. 7, the larger deviatoric stress is in the deformation history, making the residual stress increasing.

As shown in Fig. 4, in the early stages of loading and unloading tests, the compression phase of the stress-strain curve is relatively smooth. After axial loading, lateral deformation is small, and due to further axial compression, cracks are closed, crystals experience elastic deformation, axial strain changes significantly, and volumetric deformation increases. During unloading, due to the resisting effect of friction, closed fractures fail to open, and very little volumetric deformation of the rock sample was recovered after unloading (Fig. 8). In the elastic stage, the relationship between the stress and strain is linear; both axial and lateral strain linearly increases with stress. When the stress increases to approximately 70% of the yield stress, the weaker material gradually yields, internal fissures continue to form, develop and link, structural effects of macro-slip along the main fracture plane occur in the interior of the rock sample. And then the axial stress-strain curve begins to become nonlinear, lateral strain increases rapidly, and the volume begins to expand. When the stress reaches the ultimate bearing capacity of rock samples at the failure stage, lateral strain increases sharply, and the ratio of lateral strain to axial strain is greater than 1.5. Axial and lateral deformation changes in a sample at this phase because internal cracks slide and open along the main fracture plane.

The tensile strength of rock salt is very low, about 1~2 MPa (Liu *et al.* 2011). Under uniaxial compression, the rock salt began to crack or shear at the boundary between the grains. As observed in Fig. 9 (the sample after the peak strength), the failure mode of rock salt under uniaxial compression is primarily tensile-shear failure. The fracture plane is irregular and develops along the grain boundary. For the triaxial test with a confining pressure of 20 MPa, as shown in Fig. 10, after the test, the sample had no obvious macro-cracks, but numerous, inconspicuous tiny cracks are observed at grain boundaries, and also with some transgranular cracks. Crack initiation occurs at the boundaries of small grains, while confining pressure prevents micro-crack convergence, making it difficult to produce the main crack.



(a: before test, b: after test)

Fig. 9 Rock salt sample before and after an axial compression test (50 mm × 100 mm cylinders)



(a: before test, b: after test)

Fig. 10 Rock salt sample before and after a triaxial compression test under 20 MPa confining pressure (50 mm × 100 mm cylinders)

4. Damage analysis of rock salt in the cyclic loading

Damage is the result of external loading, and the degradation of the material or structure is caused by the defects within the sample micro-structure (such as micro-cracks, micro-voids, etc.). For the analysis of the mechanical behaviour of materials under stress with damage mechanics theory, the most important aspect is to select the appropriate damage definition to describe the damage state of materials. The damage variable of cyclic loading procedure is defined. The damage described as metal creep constitutive relation

$$D = 1 - \frac{\tilde{E}}{E} \quad (1)$$

Where E is elastic modulus of the undamaged material, and \tilde{E} is the elastic modulus of the damaged material. For a sample with no damage, $D = 0$; for samples that have completely lost bearing capacity, $D = 1$. D varies between $0 < D < 1$, corresponding to different damage states.

The deformation modulus of an elastic-plastic material in an instantaneous damage state and unloading stiffness have changing relationships, and thus, utilising this relationship can still describe and measure the damage behaviour of elastic-plastic materials according to the definition of the hypotheses. As shown in Fig. 11, the instantaneous deformation modulus is

$$\tilde{E} = \frac{\sigma}{\varepsilon} \quad (2)$$

The unloading stiffness E' is

$$E' = \frac{\sigma}{\varepsilon - \varepsilon'} \quad (3)$$

Where ε' is the irreversible plastic deformation after unloading. Combining Eqs. (2)-(3) gives

$$\tilde{E} = \frac{\varepsilon - \varepsilon'}{\varepsilon} E' \quad (4)$$

Substituting Eq. (4) in Eq. (1), the damage variable is given by

$$D = 1 - \frac{\varepsilon - \varepsilon'}{\varepsilon} \left(\frac{E'}{E} \right) \quad (5)$$

This formula considers the effects of irreversible plastic deformation on the definition of damage in elastic-plastic material under one-dimensional conditions. For elastic-plastic material, E' and E are the unloading stiffness and initial elastic modulus, respectively. From the previous analysis, the modulus derived from the slope of the initial loading curve is significantly less than the real elastic modulus of rock salt determined from triaxial compression tests. Thus, if the slope of the initial loading curve were used as the initial modulus, it would be significantly underestimating the elastic modulus of the material. Therefore, the unloading elastic modulus for deviatoric stress of 5 MPa should be used as the initial elastic modulus E . The evolution of damage variables under different confining pressure conditions is obtained by Eq. (5), as shown in Fig. 12.

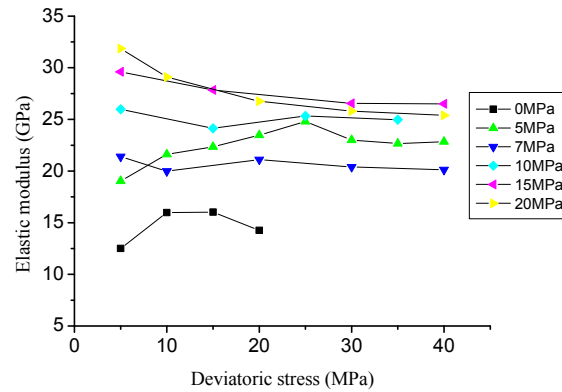


Fig. 11 Damage evolution of rock salt under different confining pressures

Micro-crack formation and expansion in rock damage evolution lead to the expansion of volume. Fig. 8 shows the volume strain curve. The volume of rock was compressed at the beginning of deformation and then expanded. We can thus conclude that during the loading process, the impact of a damage threshold effect on rock damage state should be considered. Cracks initiate only after the rock damage reaches a certain threshold and the damage state develops along with the loading. Regardless of the crack closure stress, the damage threshold has a linear relationship with the confining pressure (Ma *et al.* 2013).

5. Conclusions

The cyclic loading and unloading test of rock salt was conducted by simulating the surrounding rock of gas storage under gas pressure conditions. The elastic-plastic deformation behaviour of rock salt, the change of mechanical parameter and the effect of confining pressure on mechanical parameters were investigated. On the basis of damage mechanics theory, we described damage evolution during cyclic loading and unloading. The main conclusions are as follows:

- The curve of the sample during cyclic loading and unloading inosculates with the complete stress-strain curve in the process of monotonic loading. Even under low stress, the irreversible deformation of rock salt is large. With increasing displacement, plastic deformation was increased. The proportion of irreversible strain accounting for total deformation increases. The unloading process is described by the nonlinear elastic model, and the reloading process exhibits more elastic characteristics. The loading and unloading path of the rock sample cannot be completely repeated. There is no one-to-one correspondence between stress and strain, but always a hysteresis loop in the stress-strain curves of loading and unloading. The stress relaxation stage of the stress drop can be used for the measurement of residual stress. With increasing deviatoric stress, the internal residual stress of rock salt increases.
- During the uniaxial compression of rock salt, tensile cracking or shear slip from the boundary between grains occurs first. The failure mode of rock salt under uniaxial conditions is tensile-shear failure; the fracture plane is not planar but develops amidst twists and turns along the grain boundaries. The damage threshold has a linear relationship with the confining pressure.

Acknowledgments

The research in this paper was financially supported by the National Natural Science Foundation of China (Grant No. 51304256; 51574048), the China Postdoctoral Science Foundation (Grant No. 2013M540620; 2015T80857), the PCSIRT (NO. IRT13043), and Chongqing science and technology commission (Grant No. cstc2015jcyjA90011).

References

- Alkan, H. (2009), "Percolation model for dilatancy-induced permeability of the excavation damaged zone in rock salt", *Int. J. Rock Mech. Min. Sci.*, **46**(4), 716-724.
- Alkan, H., Cinar, Y. and Pusch, G. (2007), "Rock salt dilatancy boundary from combined acoustic emission and triaxial compression tests", *Int. J. Rock Mech. Min. Sci.*, **44**(1), 108-119.
- Chen, J., Jiang, D.Y., Ren, S. and Yang, C.H. (2015), "Comparison of the characteristics of rock salt exposed to loading and unloading of confining pressures", *Acta Geotechnica*, **11**(1), 221-230.
DOI: 10.1007/s11440-015-0369-9
- Deng, J.Q., Yang, Q. and Liu, Y.R. (2014), "Time-dependent behaviour and stability evaluation of gas storage caverns in salt rock based on deformation reinforcement theory", *Tunn. Undergr. Space Technol.*, **42**, 277-292.
- Ezersky, M. and Goretsky, I. (2014), "Velocity-resistivity versus porosity-permeability inter-relations in Dead Sea salt samples", *Eng. Geol.*, **183**, 96-115.
- Fuenkajorn, K. and Phueakphum, D. (2010), "Effects of cyclic loading on mechanical properties of Maha Sarakham salt", *Eng. Geol.*, **112**(1-4), 43-52.
- Guo, Y., Yang, C. and Fu, J. (2012), "Experimental research on mechanical characteristics of salt rock under triaxial unloading test", *Rock Soil Mech.*, **33**(3), 725-738.
- Kwon, S., Lee, C.S., Cho, S.J. and Jeon, S.W. (2009), "An investigation of the excavation damaged zone at the KAERI underground research tunnel", *Tunn. Undergr. Space Technol.*, **24**(1), 1-13.
- Li, Y., Liu, W. and Yang, C. (2014), "Daemen Experimental investigation of mechanical behavior of bedded rock salt containing inclined interlayer", *Int. J. Rock Mech. Min. Sci.*, **69**, 39-49.
- Liu, J., Xu, J. and Yang, C. (2011), "Mechanical characteristics of tensile failure of salt rock", *Chinese J. Geotech. Eng.*, **33**, 580-586.
- Liu, W., Li, Y., Yang, C., Daemen, J.J.K., Yang, Y. and Zhang, G.M. (2015), "Permeability characteristics of mudstone cap rock and interlayers in bedded salt formations and tightness assessment for underground gas storage caverns", *Eng. Geol.*, **193**, 212-223.
- Ma, L., Liu, X. and Wang, M. (2013), "Experimental investigation of the mechanical properties of rock salt under triaxial cyclic loading", *Int. J. Rock Mech. Min. Sci.*, **62**, 34-41.
- Ren, S., Bai, Y.M. and Zhang, J.P. (2013), "Experimental investigation of the fatigue properties of salt rock", *Int. J. Rock Mech. Min. Sci.*, **64**, 68-72.
- Wang, G., Zhang, L. and Zhang, Y. (2014a), "Experimental investigations of the creep-damage-rupture behaviour of rock salt", *Int. J. Rock Mech. Min. Sci.*, **66**, 181-187.
- Wang, J.B., Liu, X.R., Liu, X.J. and Huang, M. (2014b), "Creep properties and damage model for salt rock under low-frequency cyclic loading", *Geomech. Eng., Int. J.*, **7**(5), 569-587.
- Wang, T., Yang, C.H. and Yan, X. (2014c), "Dynamic response of underground gas storage salt cavern under seismic loads", *Tunn. Undergr. Space Technol.*, **43**, 241-252.
- Wisetsaen, S., Walsri, C. and Fuenkajorn, K. (2015), "Effects of loading rate and temperature on tensile strength and deformation of rock salt", *Int. J. Rock Mech. Min. Sci.*, **73**, 10-14.
- Závada, P., Desbois, G. and Urai, J.L. (2015), "Impact of solid second phases on deformation mechanisms of naturally deformed salt rocks (Kuh-e-Namak, Dashti, Iran) and rheological stratification of the Hormuz Salt Formation", *J. Struct. Geol.*, **74**, 117-144.

- Zhang, H.W., Wang, Z. and Zheng, Y. (2012), "Study on tri-axial creep experiment and constitutive relation of different rock salt", *Safety Sci.*, **50**(4), 801-805.
- Zhou, H., Wang, C. and Mishnaevsky, L. (2013), "A fractional derivative approach to full creep regions in salt rock", *Mech. Time-Depend. Mater.*, **17**(3), 413-425.

CC